JPP Journal of Pharmacy and Pharmacology

JPP 2008, 60: 1591–1600

Received May 21, 2008
Accepted August 11, 2008
DOI 10.1211/jpp/60.12.0004
ISSN 0022-3573

Comparison of chitosan nanoparticles and chitosan hydrogels for vaccine delivery

Sarah Gordon, Anne Saupe, Warren McBurney, Thomas Rades and Sarah Hook

Abstract

In this work the potential of chitosan nanoparticles (CNP) and thermosensitive chitosan hydrogels as particulate and sustained release vaccine delivery systems was investigated. CNP and chitosan hydrogels were prepared, loaded with the model protein antigen ovalbumin (OVA) and characterised. The immunostimulatory capacity of these vaccine delivery systems was assessed in-vitro and in-vivo. Particle sizing measurements and SEM images showed that optimised OVA-loaded CNP had a size of approximately 200 nm, a polydispersity index < 0.2, and a positive zeta-potential of approximately 18 mV. The amount of OVA adsorbed onto CNP was high with an adsorption efficacy of greater than 96%. Raman spectroscopy indicated conformational changes of OVA when adsorbed onto the surface of CNP. Uptake of the dispersions and immunological activation of murine dendritic cells in-vitro could be demonstrated. Investigation of the release of fluorescently-labelled OVA (FITC-OVA) from CNP and chitosan hydrogels in-vitro showed that approximately 50% of the total protein was released from CNP within a period of ten days; release of antigen from chitosan gel occurred in a more sustained manner, with < 10% of total protein being released after 10 days. The slow release from gel formulations may be explained by the strong interactions of the protein with chitosan. While OVA-loaded CNP showed no significant immunogenicity, formulations of OVA in chitosan gel were able to stimulate both cell-mediated and humoral immunity in-vivo.

Introduction

Nanoparticles are versatile delivery systems that have been used to administer a wide range of bioactives by a number of different routes. Small drug molecules, therapeutic peptides and proteins, antigens, oligonucleotides and DNA have all been formulated as nanoparticulate systems, with intravenous, oral and mucosal administration of such systems being documented (Pinto Reis et al 2006). Nanoparticles have shown many advantages in the areas of drug protection, transport and delivery (Soppimath et al 2001). Such advantages include the capacity to cross biological barriers, to protect macromolecules from degradation and to deliver drugs or macromolecules to a target site with subsequent controlled release of the bioactive material (Kayser et al 2003). As well as their application and considerable advantages in the area of drug delivery, nanoparticles can also be utilised for the delivery of vaccines. As vaccine delivery systems, nanoparticles allow for more effective delivery of antigen to antigen-presenting cells (Perrie et al 2004; Demana et al 2005; Mohammed et al 2006; White et al 2006), and provide a mechanism for the combined delivery of antigens and adjuvants and the potential for targeting to specific immune competent cells (Kreuter 1996; Clements et al 2004; Saupe et al 2006; Vangala et al 2007). Modern peptide and protein subunit vaccines are frequently poorly immune-stimulating, hence the need for use of adjuvants (O'Hagan et al 2001; Avramidis et al 2002; Bramwell & Perrie 2005; Saupe et al 2006). Also for this reason, a degree of intrinsic nanoparticle immunogenicity is desirable.

Hydrogels are another promising class of delivery systems for biomedical applications (Ishihara et al 2006). They contain only small amounts of polymeric material (1–20% in aqueous solvent), have a high molecular permeability, low interfacial tension and mechanical properties that resemble physiological soft tissue (Gupta et al 2002). These properties, combined with the ability of hydrogels to facilitate sustained release, make them interesting for both drug and vaccine delivery. In the case of vaccines, delivery of antigen in a sustained manner has been

School of Pharmacy, University of Otago, P.O. Box 913, Dunedin, New Zealand

Sarah Gordon, Anne Saupe, Warren McBurney, Thomas Rades, Sarah Hook

Correspondence: S. Hook, School of Pharmacy, University of Otago, P.O. Box 913, Dunedin, New Zealand. E-mail: sarah.hook@otago.ac.nz

Acknowledgements and funding: This research was supported by funding from the Cancer Society of New Zealand and the University of Otago. S. G. also gratefully acknowledges the University of Otago for the provision of a University of Otago Postgraduate Scholarship.

shown to be advantageous, as the resulting prolonged antigen presentation and extended interaction time with cells of the immune system can increase the likelihood of an effective immune response being generated (Lofthouse 2002). Additionally, sustained release vaccine delivery systems may enable a reduction in multiple immunisations, leading to a decrease in the cost of immunisation programmes and an increase in compliance with immunisation courses (Zhao & Leong 1996).

Chitosan is a polymer of glucosamine and *N*-acetylglucosamine derived by the partial depolymerisation of chitin, a natural component of crustacean shells. It is an inexpensive, biodegradable, non-toxic polysaccharide, demonstrated to be compatible with soft tissue in a range of toxicity tests (Qin et al 2006). Chitosan is approved by the US Food and Drug Administration (FDA) for both internal consumption and injection and has been used in a variety of foods, cosmetics, personal care products and pharmaceuticals (Dufes et al 2004; Chae et al 2005; Silva et al 2005; Qin et al 2006). Chitosan has a positive charge due to the weakly basic amino groups of the *N*-acetyl-D-glucosamine monomers. This is an advantage in that it can interact with negatively charged sites on cell surfaces. It is also able to alter tight junctions, thereby enhancing the paracellular uptake of peptides and proteins (Prego et al 2005; Amidi et al 2006). Chitosan can be formulated into micro- or nanoparticles by precipitation (Agnihotri et al 2004). Chitosan suspensions and chitosan micro- and nanoparticles have been reported to exhibit immune-stimulating activity, such as increasing accumulation and activation of macrophages and polymorphonuclear cells, suppressing tumour growth, and enhancing cytotoxic T lymphocyte (CTL) responses and delayed type hypersensitivity (DTH) (Nagamoto et al 2004; Vila et al 2004; Foged et al 2005; Luzardo-Alvarez et al 2005; Porporatto et al 2005). Antigens co-administered with, or bound to, the polysaccharide showed improved mucosal and systemic humoral immune responses, although the mechanism for this is poorly understood.

In addition to being able to be formulated as micro- and nanoparticles, chitosan can be formulated as hydrogels, either by self-association or by covalent cross linking (Agnihotri et al 2004). As well as having the general advantages of this class of delivery system mentioned above, chitosan hydrogels have the additional benefit of a positive charge. This can facilitate the entrapment of anionic moieties, such as most antigens and adjuvants. It has been found that the addition of polyol salts (such as glycerol 2-phosphate disodium hydrate) can cause conversion of purely pH-dependent, gel-forming chitosan solutions into temperature-controlled, pH-dependent gel-forming solutions (Shu & Zhu 2000; Cho et al 2005; Lopez-Leon et al 2005; Mao et al 2006). This allows solutions of chitosan to remain liquid at room temperature and transform into gels when heated to body temperature, creating an injectable depot system for sustained release of drugs and vaccines in-vivo (Berger et al 2005; Obara et al 2005; Han et al 2006). The injectability and biodegradability of such a depot system has the further benefit of eliminating the need for additional surgery to insert and remove the vaccine carrier (Jeong et al 2002).

In light of the advantages associated with administering vaccine antigen in either a particulate form or a sustained manner, the aims of this study were, firstly, to prepare and characterise both a particulate delivery system with a high antigen loading capacity and strong immunogenicity and a depot system that demonstrated both sustained release of antigen and immune-stimulating ability and, secondly, to compare the efficacy of these systems as vaccine delivery systems. Formulations consisted of chitosan nanoparticles (CNP) and thermosensitive chitosan hydrogels both loaded with the model protein ovalbumin (OVA).

Materials and Methods

Mice

Male C57Bl/6 and OT-I and OT-II transgenic mice were bred and housed under specific pathogen-free conditions at the HTRU, Dunedin, New Zealand. OT-I transgenic mice primarily express H-2K^b restricted CD8$^+$ T cells, which recognise the OVA peptide SIINFEKL ($OVA_{257–264}$), whereas OT-II transgenic mice have a high proportion of CD4$^+$ T cells with a T cell receptor (TCR) specific for the $OVA_{323–339}$ peptide (Barnden et al 1998). All mice were 6–8 weeks of age, and had free access to food and water. All animal experiments were approved by the University of Otago Animal Ethics Committee.

Preparation of chitosan nanoparticles (CNP)

CNP spontaneously formed by a precipitation/coacervation method facilitated by sodium sulfate. Briefly, 100 mg chitosan (MW 50 000–190 000 Da (based on viscosity), degree of deacetylation 75–85%; Sigma, Australia) was dissolved in a 4% v/v glacial acetic acid solution containing 2% w/v polyoxyethylene sorbitan monooleate (Tween 80) and the resulting solution filtered through a 0.22-μm filter. Nanoparticles were formed by adding a 10% w/v sodium sulfate solution drop-wise to the chitosan solution under stirring and sonication for 2 h. Before use or loading, CNP were centrifuged twice at approximately 3400 *g* for 20 min at 25°C (Heraeus Multifuge 3L; Kendro Laboratory Products, Germany).

Loading of CNP

Chitosan particles were loaded with fluorescein isothiocyanate-coupled OVA (FITC-OVA) prepared as described previously (Könnings et al 2002) or OVA (Grade V, purity approximately 98%; Sigma, Australia) by incubating 100 mg chitosan in a 20% (w/w of chitosan) aqueous FITC-OVA or OVA solution at 4°C for 12 h. Unbound FITC-OVA or OVA was removed by centrifuging the particles twice as described above. The resulting FITC-OVA-CNP or OVA-CNP dispersions were frozen and freeze-dried for 48 h (Freezone 6 freeze-dryer; Labconco, MO, USA).

Determination of entrapment efficiency

Percentage adsorption of FITC-OVA onto nanoparticles was calculated from the difference between the total amount of model protein incubated with CNP and the unbound amount of protein.

Unbound FITC-OVA was quantified by subjecting the clear supernatant of centrifuged nanoparticles dispersed in phosphate-buffered saline (PBS, pH 7.4) to fluorescence intensity measurements (RF540, Shimadzu, Japan) using an excitation and emission wavelength of 498 nm and 519 nm, respectively.

Particle size and zeta-potential measurements

Particle size, polydispersity index and zeta-potential were measured by photon correlation spectroscopy (PCS) and electrophoretic mobility in 1 mM NaCl (Zetasizer 4; Malvern Instruments Ltd, UK). Values were calculated as the average of 20 measurements of each of three independent samples.

Cryo-field emission scanning electron microscopy (Cryo-FESEM)

Morphology of both CNP and chitosan hydrogels was examined using cryo-FESEM. A drop of dispersion was filled into brass rivets and plunge-frozen in a nitrogen slush. Samples were then stored in liquid nitrogen and transferred into the cryo-stage (Alto 2500; Gatan, UK) of the microscope (JSM-6700F; JEOL, Japan). Samples were fractured on the cryo-stage and coated with platinum. Images were acquired at a temperature of −140°C and a voltage of 2.5–3.0 kV.

Raman spectroscopy

Raman spectroscopy was used to obtain further information on the binding of OVA onto the surface of CNP by comparing OVA-loaded CNP to physical mixtures of CNP and OVA. FT-Raman spectra were collected using a Bruker IFS-55 interferometer with an FRA/106 S attachment. The excitation source was an Nd:YAG laser with an excitation wavelength of 1064 nm. A liquid-nitrogen-cooled Ge diode (D-418) was used to detect Raman photons. All spectra were taken with a laser power of 300 mW, over a 1-h period at a resolution of 4 cm^{-1}. Spectra were analysed using GRAMS 5.0 (Galactic Industries, NH, USA).

In-vitro immunological characterisation of the immune-stimulating capacity of OVA-loaded CNP

Murine bone-marrow-derived dendritic cells (bmDC) were generated as previously described (White et al 2006). Following 48 h of pulsing bmDC with titrated amounts of CNP loaded with OVA labelled with a fluorescent tag (FITC) and unloaded CNP with no fluorescent tag, uptake of formulation and activation of bmDC was measured by flow cytometry. Cells were stained with antibodies directed against the dendritic cell marker CD11c and the activation markers CD86 and MHC class II (BD Pharmingen, Franklin Lakes, NJ, USA) before carrying out flow cytometry (FACScalibur; Becton Dickinson, NJ, USA). Data gained was analysed using CellQuest Pro (Becton Dickinson).

Preparation of thermosensitive chitosan hydrogels

Hydrogels were made by dissolving different concentrations of chitosan (2–3% w/v) in dilute aqueous hydrochloric acid (0.05–0.1 M). While in an ice bath, an aqueous solution of glycerol 2-phosphate disodium hydrate (GP, 5.6–6% w/v) was added drop-wise to the chitosan solution. FITC-OVA or OVA was then dissolved in the chitosan solution. The chitosan/GP solution was transformed into a hydrogel by increasing the temperature to 37°C.

Viscosity

Viscosity of the hydrogels was measured using a Brookfield DVIII viscometer (Brookfield Engineering Laboratories, MA, USA) fitted with a CP-42 cone spindle. Measurements were carried out in triplicate at 25°C and 37°C.

Determination of in-vitro release

Release of FITC-OVA from both CNP and 2.4% chitosan hydrogels, each containing 20% FITC-OVA, was determined. Samples consisting of 250 μg of CNP and 1 mL of chitosan hydrogel both in 2 mL of PBS (pH 7.4) were covered and incubated at 37°C for 10 days. At various time points, 100 μL of buffer was removed from each sample (replaced with an equal volume of fresh buffer) and centrifuged. The fluorescence intensity of the resulting supernatants was then determined as described above. FITC-OVA release (%) at each time point was calculated from the measured fluorescence intensity using an FITC-OVA standard curve. Standard curves were constructed at each time point from a FITC-OVA stock solution stored together with the samples at 37°C. The pH of release samples and FITC-OVA stock solution was monitored over the course of the release study and showed no significant deviation from pH 7.4.

In-vivo immunological characterisation of OVA-loaded CNP and chitosan hydrogels

Adoptive transfer of OT-I and OT-II transgenic T cells into C57Bl/6 mice was performed on day −1 of experimentation. Briefly, the spleen, axial and brachial lymph nodes were harvested from OT-I and OT-II transgenic mice. Single-cell suspensions (8×10^6 cells/mL) were prepared in sterile PBS and 500 μL of mixed OT-I and OT-II cells were injected via the tail vein into C57Bl/6 mice.

On day 0, mice were immunised with thermally-sensitive chitosan solution containing 20 μg OVA, resulting in the formation of a gel depot, or 50 μg CNP loaded with 10 μg OVA, in sterile PBS. Control groups received either 10 μg OVA in sterile PBS or 10 μg OVA in alum. Control and CNP groups were given further booster immunisations on day 14. All formulations were 200 μL in volume and were administered subcutaneously in the scruff of the neck. On day 28, all mice were pulsed with 10 μg OVA to maximise the observed immune response.

Mice were culled on day 30. Draining lymph nodes were collected and the cells isolated and stained for analysis by flow cytometry. Cells were incubated firstly with anti-CD16/CD32 antibody (to block non-specific binding to cell surfaces), followed by antibodies directed against either the cytotoxic T cell marker CD8 or the helper T cell marker

CD4, as well as the transgenic T cell markers Vα2 and Vβ5.1 (BD Pharmingen). OVA-specific IgG titres were determined by ELISA (Myschik et al 2008).

Statistical analysis

Where applicable, results are expressed as mean ± s.d. Statistical analysis was carried out using a one-way analysis of variance using SPSS 14.0, release 14.0.0 (SPSS Inc., Chicago, IL, USA) followed by a post-hoc analysis using Tukey's pairwise comparison.

Results and Discussion

Optimisation of particle formation

To achieve optimal nanoparticle formation and antigen loading it was necessary to titrate the concentration of sodium sulfate added to the chitosan solution. Different amounts of sodium sulfate were added drop-wise during the precipitation step to a final concentration in the range 0.1–0.4%. Concentrations higher than 0.4% led to gel formation at room temperature as observed macroscopically and by cryo-FESEM (Figure 1A, Table 1). Microparticles were formed using 0.15–0.4% sodium sulfate (Figure 1B, Table 1). Addition of 0.1% sodium sulfate resulted in nanoparticles with an average diameter of 102 ± 13 nm and a zeta-potential of 28.8 ± 0.1 mV (Figure 1C, Table 1). The polydispersity index of all samples measured directly after preparation was consistently < 0.2, indicating a uniform size distribution of the chitosan nanoparticles. A concentration of 0.1% was therefore considered as the optimal sodium sulfate concentration for CNP formation. Long-term stability investigation suggested that the dispersions remained in the nanometre range over the investigated period of 30 days (particle size at day 30: 132 ± 36 nm).

Adsorption of FITC-OVA to CNP

The adsorption efficacy of FITC-OVA to chitosan particles was > 90% for salt concentrations of $\leq$ 0.2% sodium sulfate, independent of particle size (Table 1). Adsorption of FITC-OVA to CNP was rapid, occurring within 30 min, and can be attributed to ionic interactions between the negatively charged protein and the cationic CNP. The amount of FITC-OVA adsorbed onto nano-sized chitosan particles was high (most likely reflecting the larger surface area of such particles), with an adsorption efficacy of > 96%. This value is similar to that seen in the study of Amidi et al (2006). Adsorption of antigen onto CNP gave the particles a rough surface (Figure 1D), increased the size of the particles to 226 ± 38 nm (with no observed increase in polydispersity index) and decreased the zeta-potential of the particles to + 18.3 ± 1.8 mV. Aggregation of particles as a result of this decrease in surface charge led to an increase in particle size over time (size of FITC-OVA-loaded particles at day 14: 1449 ± 155 nm). The addition of FITC-OVA to particles therefore resulted in a reduction in long-term stability relative to that of unloaded chitosan nanoparticles.

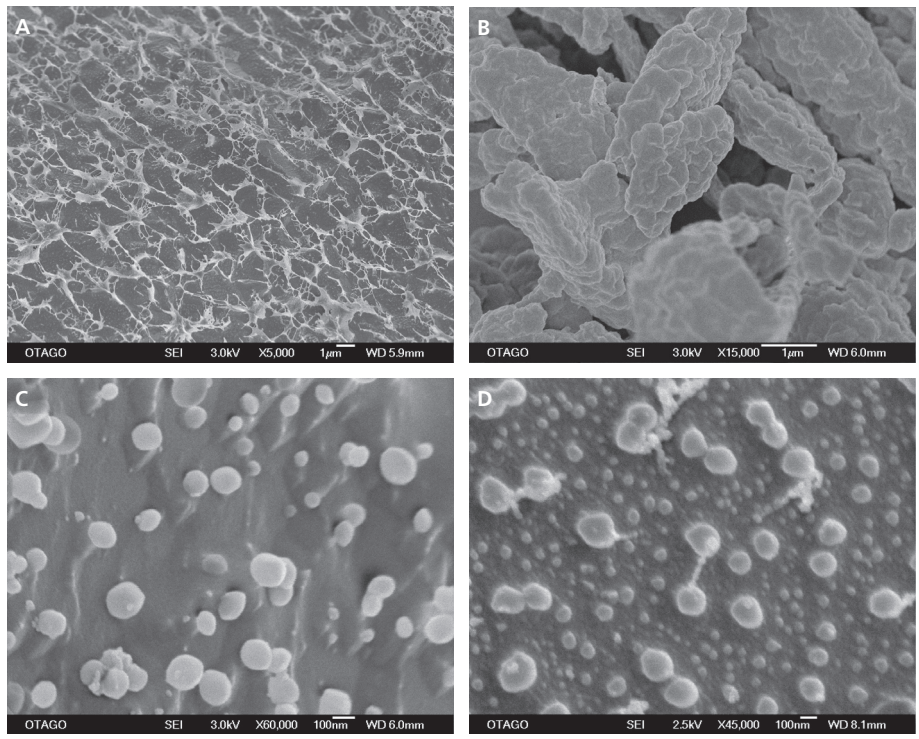

Figure 1 Cryo-FESEM images of chitosan formulations made with titrated concentrations of sodium sulfate and after loading with antigen. Representative micrographs of formulations made with greater than 0.4% sodium sulfate (A), formulations made with 0.15–0.4% sodium sulfate (B), formulations made with 0.1% sodium sulfate (C) and formulations made with 0.1% sodium sulfate and loaded with FITC-OVA (D).

Table 1 Particle size, zeta-potential and amount of adsorbed FITC-OVA as a function of final % w/v sodium sulfate concentration

Na_2SO_4 (final % w/v)	Unloaded		Loaded	
	Average diameter (nm)	Zeta-potential (mV)	Adsorbed OVA (%)	CNP:OVA ratio
0.4	Gel	–	–	–
0.3	3182 ± 217	25.1 ± 0.3	53 ± 7	2:1
0.2	1660 ± 195	25.7 ± 0.1	90 ± 1	2:1
0.2	1660 ± 195	25.7 ± 0.1	95 ± 0.3	4:1
0.15	905 ± 67	24.6 ± 0.2	97 ± 0.5	5:1
0.1	102 ± 13	28.8 ± 0.1	96 ± 1	5:1

Data are shown as the mean ± s.d. of 3 experiments.

Raman spectroscopy

Raman difference spectroscopy is a sensitive tool for detecting structural changes in large macromolecular complexes (Tuma 2005). The Raman spectrum of a protein is dominated by bands associated with the peptide main chain, and aromatic and sulfur-containing side chains. In this study, Raman spectroscopy was carried out to determine whether adsorption of OVA to CNP resulted in conformational changes to the protein. Such changes may affect the ability of the vaccine to generate protective antibody responses (Ulbrandt et al 2001; Paster et al 2002).

Raman spectra were obtained from chitosan, CNP, OVA bulk material, physical mixtures of CNP and OVA powders (5:1 w/w mixtures of chitosan to OVA in the solid state), and OVA-loaded CNP (5:1 w/w of CNP to OVA) (Figure 2). If two macromolecules interact physico-chemically, the Raman spectra will be different from the addition spectra of the two pure components or of a simple physical mixture. These differences can originate from interactions such as hydrogen bonding as well as ion–ion and ion–dipole interactions, indicating conformational changes in the protein structure. These changes result in band shifts, intensity changes and line broadening (Yamasaki et al 2003).

Spectra were analysed for changes in the OVA-specific bands that occurred when OVA was physically mixed with CNP and when it was loaded onto CNP. The spectral region around 1665 cm^{-1} (Figure 2) is dominated by the conformation-sensitive amide I and amide II bands. OVA-specific bands were visible in the pure OVA sample and in the physical mixture spectra. The intensity of these bands was lower in the physical mixture, as only 20% of this sample consisted of OVA. In contrast, no amide bands were observed in the Raman spectrum of the OVA-loaded CNP, indicating the occurrence of conformational changes to OVA when adsorbed onto the surface of CNP.

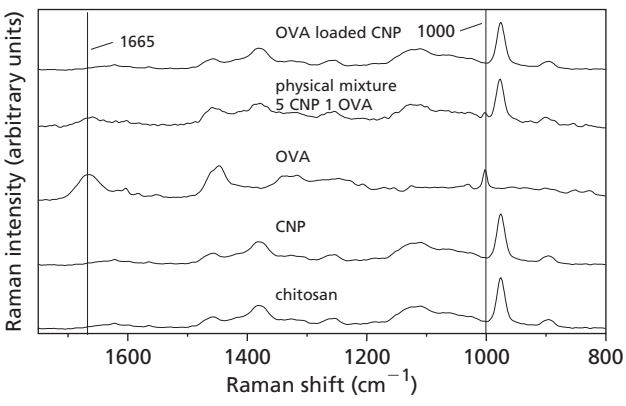

Figure 2 Raman spectra of OVA-loaded CNP (5:1 ratio of CNP to OVA), physical mixture of CNP and OVA (5:1 ratio), OVA, CNP and chitosan. Spectral regions around 1665 cm^{-1} and 1001 cm^{-1} where differences were observed between the OVA-loaded CNP and the physical mixture of CNP with OVA have been indicated with a line.

Furthermore, the phenylalanine band at 1001 cm^{-1}, which was visible in the pure OVA sample and the physical mixture (again at a lower intensity), was absent in the OVA-loaded CNP sample.

These results indicate that indeed a conformational change is taking place when OVA is loaded onto the CNP. As it has been shown that conformational changes may affect the quality of the immune responses generated by a vaccine (Wang 1999), immunological studies of T- and B-cell responses to OVA-loaded CNP will be required to discover if this is true for the current formulation.

In-vitro immunological characterisation of the immune-stimulating capacity of FITC-OVA-loaded CNP

Previous studies have shown that CNP are immunostimulatory both in-vitro and in-vivo (Seferian & Martinez 2001; Read et al 2005). CNP loaded with FITC-OVA and unloaded CNP were incubated with murine bmDC to determine whether dendritic cells could take up CNP and subsequently become activated. When murine bmDC were incubated with increasing amounts of CNP loaded with FITC-OVA, significant uptake of FITC-OVA-loaded CNP could be demonstrated ($P \leq 0.01$, Figure 3A). Activation was then determined by examining expression of the activation markers CD86 and MHC class II on bmDC incubated with either CNP or FITC-OVA-loaded CNP (Figure 3B, C). Expression of the activation markers increased in a concentration-dependent manner on cells when incubated with both CNP and FITC-OVA-loaded CNP, although this increase was only significantly higher than background levels for bmDC incubated with high concentrations of unloaded CNP. The immunostimulatory effect of unloaded CNP was not observed to be significantly augmented by coating the particles with antigen.

Gelation behaviour of chitosan solutions

The optimal conditions for preparing temperature-dependent chitosan hydrogels were determined. Desired properties used

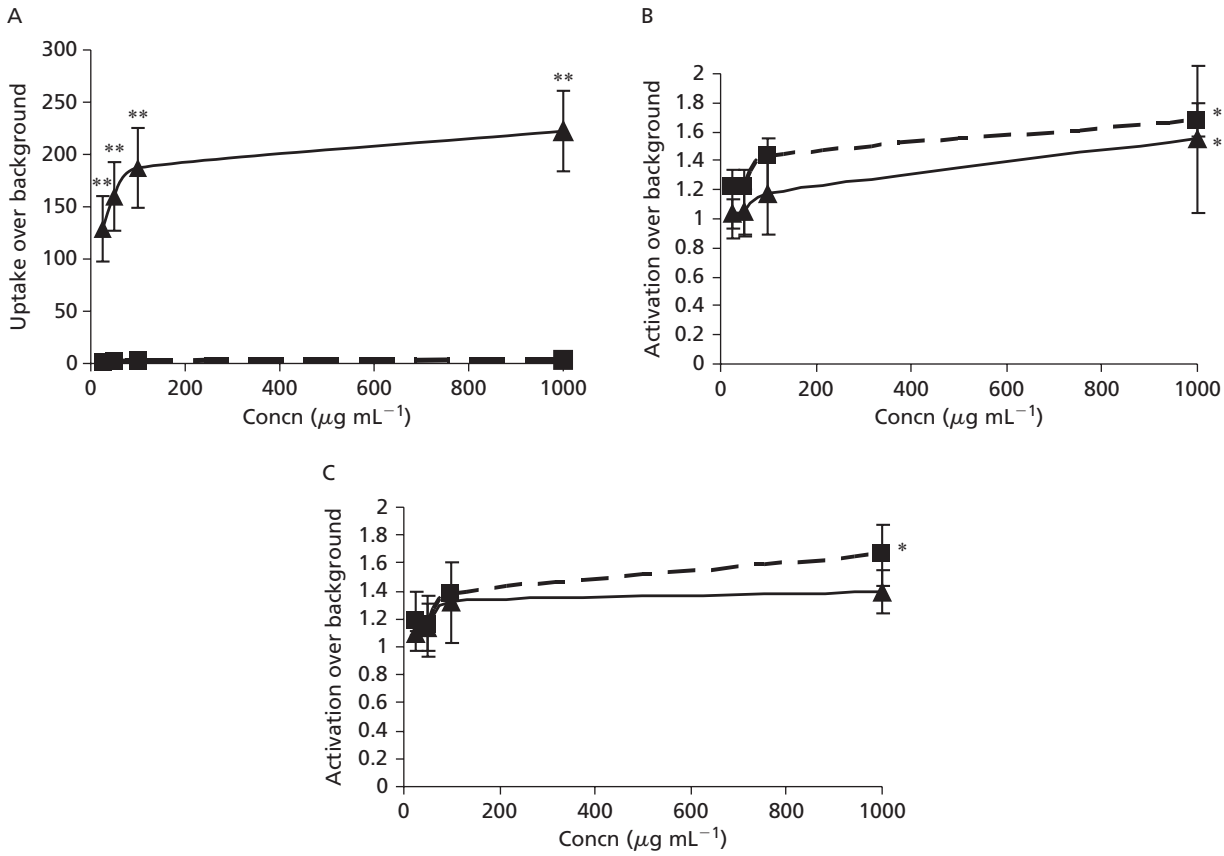

Figure 3 Uptake into and activation of murine bmDC by CNP loaded with OVA labelled with a fluorescent tag (FITC) (triangles) and unloaded CNP with no fluorescent tag (squares). Uptake of the formulations as measured by a fold increase in cell fluorescence (A), and expression of the activation markers CD86 (B) and MHCII (C) is shown. Data are shown as the mean ± s.d. from three experiments. $*P \leq 0.05$, $**P \leq 0.01$.

to define such optimal preparation conditions were being a low viscosity injectable solution at room temperature and rapid induction of gelation upon heating to body temperature. A chitosan solution was prepared in dilute hydrochloric acid and the pH maintained by varying the concentration of hydrochloric acid in which the chitosan was dissolved. The optimal conditions for gelation were 2.4% w/v chitosan dissolved in 0.1 M hydrochloric acid with the addition of 5.7% w/v GP (concentrations in final solution; data not shown). The effect of chitosan concentration and pH on gelation at either 25°C or 37°C was then analysed by determining the viscosity (Figure 4).

At 25°C and pH 6.5 (Figure 4A) the viscosities of both the 2% and 2.4% chitosan solutions were less than 1800 mPa s. The solutions flowed easily and were injectable through a 20-gauge needle. The viscosity of both solutions increased only slightly over 30 min. Increasing the pH to 6.8 (Figure 4C) led to a considerable increase in the viscosity of both solutions. However, this increase was not sufficient to induce gelation of either the 2% or 2.4% chitosan solutions.

At a chitosan concentration of 2.4%, a pH of 6.8 and a temperature of 37°C (Figure 4D), the sol–gel transformation occurred within 2 min. Decreasing the pH of the solution to 6.5 (Figure 4B) or using a lower polymer concentration of 2% (Figure 4D) meant that gelation was not achieved at 37°C within 30 min.

As mentioned above, optimal characteristics for an in-situ gelling system would be stability at room temperature and fast gelation following injection, to avoid diffusion of the antigen from the site of vaccination. Therefore the 2.4% chitosan solution formulated at a pH of 6.8 was used in all further experiments.

Physical characterisation of chitosan hydrogels

The release of active ingredients from gels is generally diffusion controlled, with diffusion being determined by the porosity of the gel and volume of the water present (Mi et al 1999; Kofuji et al 2004; Subramanian & Hommerding 2005). The shape, size and distribution of pores are also important parameters for the release of the antigen. The morphology of chitosan hydrogels (2.4% polymer) was examined by cryo-FESEM after 24 h and 24 days in PBS at 37°C (Figure 5). The hydrogel had a very fibrous structure with large interconnected areas between the fibres (Figure 5A). After 24 days of immersion in PBS, pore size had increased and the gel had a more open structure (Figure 5B). However, macroscopically

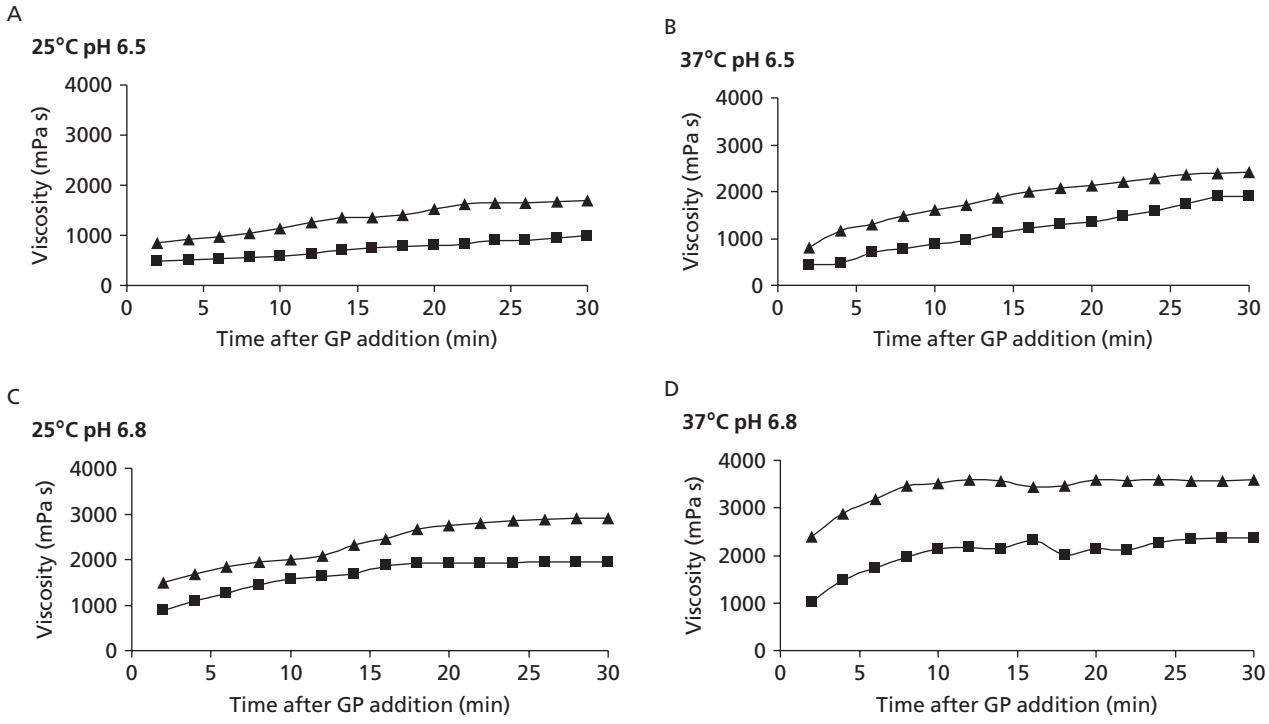

Figure 4 Viscosity of solutions containing 2% (squares) or 2.4% (triangles) chitosan following addition of glycerol phosphate (GP). The effect of pH and temperature was analysed: pH 6.5, 25°C (A), pH 6.5, 37°C (B), pH 6.8, 25°C (C), pH 6.8, 37°C (D).

the systems did not lose their gel character and remained solid over the investigated time period of 24 days.

Comparison of FITC-OVA release from CNP and chitosan gels

Release profiles of FITC-OVA from chitosan hydrogel and from FITC-OVA-loaded CNP were analysed over 10 days (Figure 6). Release of FITC-OVA from chitosan gel was seen to occur more slowly than release from CNP. At day 10, approximately 50% of the initially incorporated total protein had been released from CNP, whereas less than 10% of total protein was released from chitosan gels. The observed release of protein from the gels in fact occurred over the first 4 days, following an initial burst release in the first two days, and was not seen to increase further over the remaining duration of the study.

Such a low level of release is most likely due to soluble FITC-OVA becoming tightly bound in the chitosan hydrogel matrix due to strong electrostatic interactions. This hypothesis is supported by the aforementioned Raman data (Figure 2), which indicates the occurrence of a physico-chemical interaction between OVA and chitosan. Furthermore, the possibility of this tightly bound protein being released through erosion-controlled mechanisms is prevented, as gel degradation did not occur in this in-vitro system (Figure 5B). This explanation is supported by the findings of Ruel-Gariépy et al (2000) who observed incomplete in-vitro release of FITC-albumin from chitosan gel. In that study, a release of 50% FITC-albumin was reached at 3 days, after which a plateau in

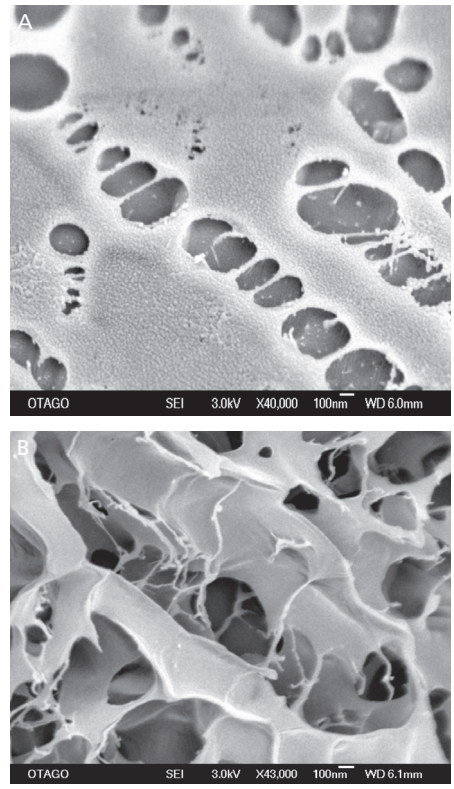

Figure 5 Cryo-FESEM images of 2.4% chitosan hydrogels containing OVA 24 h (A) and 24 days (B) after immersion in PBS at 37°C. The scale bar is 100 nm.

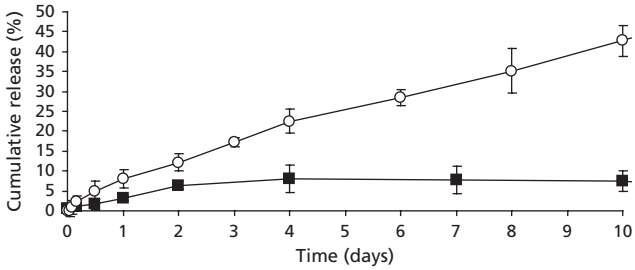

Figure 6 Cumulative release of FITC-OVA from CNP (circles) and chitosan hydrogel (squares) over 10 days, as determined by fluorescence intensity measurements. Data are shown as the mean ± s.d. of three experiments.

release occurred. A similar hypothesis of protein entrapment within the chitosan gel matrix was made, and further investigated by the addition of lysozyme to the release media to facilitate gel degradation. This resulted in release of a further 25% of FITC-albumin; 100% release was stated to be unachievable due to the inability of lysozyme to completely degrade the chitosan gel.

While erosion-controlled release of antigen does not seem to play a role in the in-vitro situation, in-vivo a number of factors, such as the action of enzymes (including lysozyme and *N*-acetyl-glucosaminidase) that have been shown to cause chitosan gel degradation (Köping-Höggård et al 2001), will affect release of antigen from chitosan gels. The low release of protein observed in-vitro is therefore not regarded as a prohibitive issue with respect to the study of the in-vivo behaviour of these systems.

In-vivo immunostimulatory ability of OVA incorporated into chitosan formulations

Investigation of the immunostimulatory ability of OVA in chitosan gel formulations in-vivo showed that a single administration of such a formulation resulted in higher percentages of both $CD8^+$ and $CD4^+$ transgenic T cells in the lymph nodes of immunised mice in comparison with the prime and boost administered OVA in PBS; however this difference was only significant in the case of $CD4^+$ T cells. The antigen-specific expansion of both $CD8^+$ and $CD4^+$ transgenic T cells in response to OVA in gel was significantly higher than that induced by a prime and boost regimen of OVA in alum (Figure 7A, B). In addition to cell activation, the ability of OVA in chitosan gel to stimulate a humoral immune response was examined through assessment of antibody production (Figure 7C). Administration

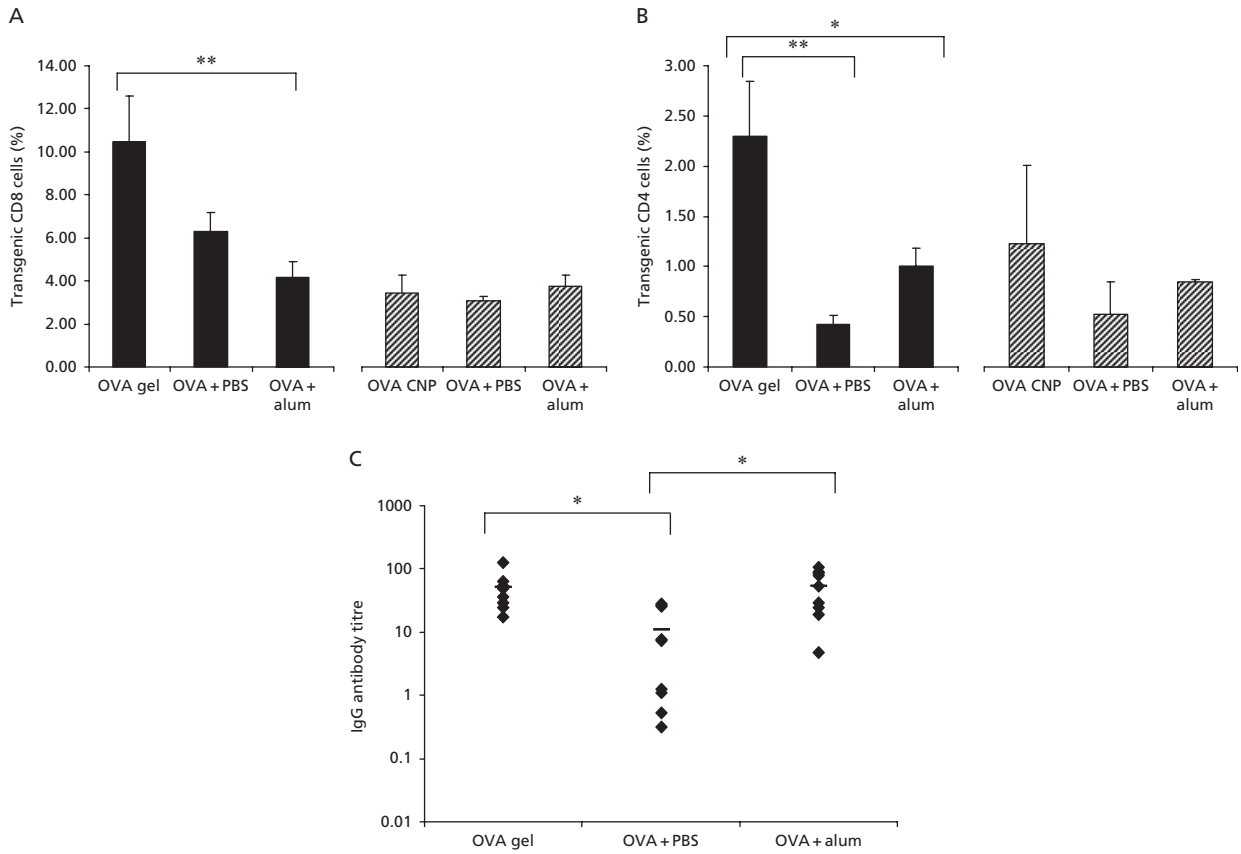

Figure 7 Activation of $CD8^+$ (A) and $CD4^+$ (B) T cells isolated from lymph nodes determined using flow cytometry (chitosan gel experiments are shown on the left, CNP experiments on the right), and production of OVA-specific IgG antibody as determined by ELISA (C). Investigation of the immunostimulatory ability of OVA gel and OVA CNP formulations was carried out in separate experiments. In both cases, T-cell activation data is from one representative experiment with n = 3 mice per group. Antibody data were pooled from three independent experiments; diamonds represent results of individual mice, bars represent mean antibody titres. $*P \leq 0.05$, $**P \leq 0.01$.

of OVA in chitosan gel was seen to result in production of significantly higher OVA-specific IgG antibody titres in comparison with the negative OVA + PBS control, and approximately equivalent titres to OVA in alum. These results are promising, as alum is known to be an effective inducer of CD4 and antibody responses but not CD8 responses (Gupta 1998). In-vivo results in general are also in accordance with the findings of Zaharoff et al (2007) who reported that administration of a viscous, depot-forming formulation of chitosan containing the model antigen β-galactosidase induced both cell-mediated and humoral immune responses.

In contrast, no significant immune activation was stimulated by OVA-loaded CNP (Figure 7A, B; IgG data not shown). This lack of observed immunostimulatory activity was unexpected, as CNP have been shown by a number of researchers to generate an effective immune response. In most of these cases, however, CNP formulations were delivered via mucosal routes (Seferian & Martinez 2001; Nagamoto et al 2004; Vila et al 2004; Porporatto et al 2005; Read et al 2005). Previously mentioned properties of chitosan, such as the ability to adhere to mucosal surfaces, may be responsible for this observed efficacy following mucosal administration; however, administration of CNP-based formulations via the subcutaneous route, as in this study, would negate this property, and may therefore explain the observed lack of immune stimulation in response to CNP administration (Zaharoff et al 2007).

As chitosan hydrogels were immunostimulatory while CNP were not, it therefore appears that chitosan can effectively induce an immune response when delivered subcutaneously if formulated to provide a sustained-release depot. This is in agreement with existing literature, which has shown that by facilitating increased exposure to antigen presenting cells, slow release of an antigen from a depot is able to enhance in-vivo immune stimulation (Zinkernagel et al 1997; Lofthouse 2002; Myschik et al 2008). It is unlikely that the lack of reactivity to antigen-loaded CNP was due to the interactions between OVA and chitosan identified in the Raman studies, as these would also have occurred in the gels.

Conclusion

Properties of CNP and chitosan-based hydrogels, loaded with the model protein antigen OVA, were studied to determine their potential for vaccine delivery applications. Optimised methods were developed for the reproducible manufacture of CNP with a defined size range. The CNP had a high loading capacity and were able to activate antigen presenting cells in-vitro. However the loading of antigen onto CNP resulted in conformational changes to the protein. The bound protein released only slowly with less than 50% being released from CNP after 10 days in-vitro incubation. In the second part of the study, an injectable thermosensitive chitosan hydrogel was prepared. The model protein OVA could be incorporated into the chitosan solution before gelation, making this an attractive system for vaccine delivery. Release of protein from chitosan gel formulations in-vitro was even slower than from CNP with less than 10% being released after 10 days. However, release in-vivo, where gel degradation can occur as a result of several factors including enzymatic hydrolysis, may be very different. In-vivo investigations showed negligible immune responses to OVA-loaded CNP formulations, possibly reflecting the fact that non-mucosal administration of such a system may not result in maximal immune responses. OVA in chitosan gel formulations resulted in the expansion of $CD8^+$ and $CD4^+$ T cells and in OVA-specific antibody production.

References

Agnihotri, S. A., Mallikarjuna, N. N., Aminabhavi, T. M. (2004) Recent advances on chitosan-based micro- and nanoparticles in drug delivery. *J. Control. Release* **100**: 5–28

Amidi, M., Romeijn, S. G., Borchard, G., Junginger, H. E., Hennink, W. E., Jiskoot, W. (2006) Preparation and characterization of protein-loaded N-trimethyl chitosan nanoparticles as nasal delivery system. *J. Control. Release* **111**: 107–116

Avramidis, N., Victoratos, P., Yiangou, M., Hadjipetrou-Kourounakis, L. (2002) Adjuvant regulation of cytokine profile and antibody isotype of immune responses to Mycoplasma agalactiae in mice. *Vet. Microbiol.* **88**: 325–338

Barnden, M. J., Allison, J., Heath, W. R., Carbone, F. R. (1998) Defective TCR expression in transgenic mice constructed using cDNA-based α- and β-chain genes under the control of heterologous regulatory elements. *Immunol. Cell Biol.* **76**: 34–40

Berger, J., Reist, M., Chenite, A., Felt-Baeyens, O., Mayer, J. M., Gurny, R. (2005) Pseudo-thermosetting chitosan hydrogels for biomedical application. *Int. J. Pharm.* **288**: 197–206

Bramwell, V. W., Perrie, Y. (2005) Particulate delivery systems for vaccines. *Crit. Rev. Ther. Drug Carrier Syst.* **22**: 151–214

Chae, S. Y., Jang, M.-K., Nah, J.-W. (2005) Influence of molecular weight on oral absorption of water soluble chitosans. *J. Control. Release* **102**: 383–394

Cho, J., Heuzey, M.-C., Begin, A., Carreau, P. J. (2005) Physical gelation of chitosan in the presence of β-glycerophosphate: the effect of temperature. *Biomacromolecules* **6**: 3267–3275

Clements, C. J., Larsen, G., Jodar, L. (2004) Technologies that make administration of vaccines safer. *Vaccine* **22**: 2054–2058

Demana, P. H., Davies, N. M., Hook, S., Rades, T. (2005) Quil A-lipid powder formulations releasing ISCOMs and related colloidal stuctures upon hydration. *J. Control. Release* **103**: 45–59

Dufes, C., Muller, J.-M., Couet, W., Olivier, J.-C., Uchegbu, I. F., Schätzlein, A. G. (2004) Anticancer drug delivery with transferrin targeted polymeric chitosan vesicles. *Pharm. Res.* **21**: 101–107

Foged, C., Brodin, B., Frokjaer, S., Sundblad, A. (2005) Particle size and surface charge affect particle uptake by human dendritic cells in an in vitro model. *Int. J. Pharm.* **298**: 315–322

Gupta, R. K. (1998) Aluminum compounds as vaccine adjuvants. *Adv. Drug Deliv. Rev.* **32**: 155–172

Gupta, P., Vermani, K., Garg, S. (2002) Hydrogels: from controlled release to pH-responsive drug delivery. *Drug Discov. Today* **7**: 569–579

Han, I.-K., Kim, Y. B., Kang, H.-S., Sul, D., Jung, W.-W., Cho, H. J., Oh, Y.-K. (2006) Thermosensitive and mucoadhesive delivery systems of mucosal vaccines. *Methods* **38**: 106–111

Ishihara, M., Obara, K., Nakamura, S., Fujita, M., Masuoka, K., Kanatani, Y., Takase, B., Hattori, H., Morimoto, Y., Ishihara, M., Maehara, T., Kikuchi, M. (2006) Chitosan hydrogel as a drug delivery carrier to control angiogenesis. *J. Artif. Organs* **9**: 8–16

Jeong, B., Lee, K. M., Gutowska, A., An, Y. H. (2002) Thermogelling biodegradable copolymer aqueous solutions for injectable protein delivery and tissue engineering. *Biomacromolecules* **3**: 865–868

Kayser, O., Olbrich, C., Croft, S. L., Kiderlen, A. F. (2003) Formulation and biopharmaceutical issues in the development of drug delivery systems for antiparasitic drugs. *Parasitol. Res.* **90**: S63–S70

Kofuji, K., Akamine, H., Qian, C. J., Watanabe, K., Togan, Y., Nishimura, M., Sugiyama, I., Murata, Y., Kawashima, S. (2004) Therapeutic efficacy of sustained drug release from chitosan gel on local inflammation. *Int. J. Pharm.* **272**: 65–78

Könnings, S., Copland, M. J., Davies, N. M., Rades, T. (2002) A method for the incorporation of ovalbumin into immune stimulating complexes prepared by the hydration method. *Int. J. Pharm.* **241**: 385–389

Köping-Höggård, M., Tubulekas, I., Guan, H., Edwards, K., Nilsson, M., Vårum, K., Artursson, P. (2001) Chitosan as a nonviral gene delivery system. Structure-property relationships and characteristics compared with polyethylenimine *in vitro* and after lung administration *in vivo*. *Gene Ther.* **8**: 1108–1121

Kreuter, J. (1996) Nanoparticles and microparticles for drug and vaccine delivery. *J. Anat.* **189**: 503–505

Lofthouse, S. (2002) Immunological aspects of controlled antigen delivery. *Adv. Drug Deliv. Rev.* **54**: 863–870

Lopez-Leon, T., Carvalho, E. L. S., Seijo, B., Ortega-Vinuesa, J. L., Bastos-Gonzalez, D. (2005) Physicochemical characterization of chitosan nanoparticles: electrokinetic and stability behavior. *J. Colloid Interface Sci.* **283**: 344–351

Luzardo-Alvarez, A., Blarer, N., Peter, K., Romero, J. F., Reymond, C., Corradin, G., Gander, B. (2005) Biodegradable microspheres alone do not stimulate murine macrophages in vitro, but prolong antigen presentation by macrophages in vitro and stimulate a solid immune response in mice. *J. Control. Release* **109**: 62–76

Mao, J., Kondu, S., Ji, H.-F., McShane, M. J. (2006) Study of the near-neutral pH-sensitivity of chitosan/gelatin hydrogels by turbidimetry and microcantilever deflection. *Biotechnol. Bioeng.* **95**: 333–341

Mi, F.-L., Shyu, S.-S., Wong, T.-B., Jang, S.-F., Lee, S.-T., Lu, K.-T. (1999) Chitosan-polyelectrolyte complexation for the preparation of gel beads and controlled release of anticancer drug. II. Effect of pH-dependent ionic crosslinking or interpolymer complex using tripolyphosphate or polyphosphate as reagent. *J. Appl. Polym. Sci.* **74**: 1093–1107

Mohammed, A. R., Bramwell, V. W., Coombes, A. G. A., Perrie, Y. (2006) Lyophilisation and sterilisation of liposomal vaccines to produce stable and sterile products. *Methods* **40**: 30–38

Myschik, J., McBurney, W. T., Hennessy, T., Phipps-Green, A., Rades, T., Hook, S. (2008) Immunostimulatory biodegradable implants containing the adjuvant Quil-A – Part II: *in vivo* evaluation. *J. Drug Target.* **16**: 224–232

Nagamoto, T., Hattori, Y., Takayama, K., Maitani, Y. (2004) Novel chitosan particles and chitosan-coated emulsions inducing immune response via intranasal vaccine delivery. *Pharm. Res.* **21**: 671–674

Obara, K., Ishihara, M., Ozeki, Y., Ishizuka, T., Hayashi, T., Nakamura, S., Saito, Y., Yura, H., Matsui, T., Hattori, H., Takase, B., Ishihara, M., Kikuchi, M., Maehara, T. (2005) Controlled release of paclitaxel from photocrosslinked chitosan hydrogels and its subsequent effect on subcutaneous tumor growth in mice. *J. Control. Release* **110**: 79–89

O'Hagan, D. T., MacKichan, M. L., Singh, M. (2001) Recent developments in adjuvants for vaccines against infectious diseases. *Biomol. Eng.* **18**: 69–85

Paster, W., Kalat, M., Zehetner, M., Schweighoffer, T. (2002) Structural elements of a protein antigen determine immunogenicity of the embedded MHC class I-restricted T cell epitope. *J. Immunol.* **169**: 2937–2946

Perrie, Y., Barralet, J. E., McNeil, S., Vangala, A. (2004) Surfactant vesicle-mediated delivery of DNA vaccines via the subcutaneous route. *Int. J. Pharm.* **284**: 31–41

Pinto Reis, C., Neufeld, R. J., Ribeiro, A. J., Veiga, F. (2006) Nanoencapsulation II. Biomedical applications and current status of peptide and protein nanoparticulate delivery systems. *Nanomedicine* **2**: 53–65

Porporatto, C., Bianco, I. D., Correa, S. G. (2005) Local and systemic activity of the polysaccharide chitosan at lymphoid tissues after oral administration. *J. Leukoc. Biol.* **78**: 62–69

Prego, C., Garcia, M., Torres, D., Alonso, M. J. (2005) Transmucosal macromolecular drug delivery. *J. Control. Release* **101**: 151–162

Qin, C., Gao, J., Wang, L., Zeng, L., Liu, Y. (2006) Safety evaluation of short-term exposure to chitooligomers from enzymic preparation. *Food Chem. Toxicol.* **44**: 855–861

Read, R. C., Naylor, S. C., Potter, C. W., Bond, J., Jabbal-Gill, I., Fisher, A., Illum, L., Jennings, R. (2005) Effective nasal influenza vaccine delivery using chitosan. *Vaccine* **23**: 4367–4374

Ruel-Gariépy, E., Chenite, A., Chaput, C., Guirguis, S., Leroux, J.-C. (2000) Characterization of thermosensitive chitosan gels for the sustained delivery of drugs. *Int. J. Pharm.* **203**: 89–98

Saupe, A., McBurney, W., Rades, T., Hook, S. (2006) Immunostimulatory colloidal delivery systems for cancer vaccines. *Expert Opin. Drug Deliv.* **3**: 345–354

Seferian, P. G., Martinez, M. L. (2001) Immune stimulating activity of two new chitosan containing adjuvant formulations. *Vaccine* **19**: 661–668

Shu, X. Z., Zhu, K. J. (2000) A novel approach to prepare tripolyphosphate/chitosan complex beads for controlled release drug delivery. *Int. J. Pharm.* **201**: 51–58

Silva, S. S., Santos, M. I., Coutinho, O. P., Mano, J. F., Reis, R. L. (2005) Physical properties and biocompatibility of chitosan/soy blended membranes. *J. Mater. Sci. Mater. Med.* **16**: 575–579

Soppimath, K. S., Aminabhavi, T. M., Kulkarni, A. R., Rudzinski, W. E. (2001) Biodegradable polymeric nanoparticles as drug delivery devices. *J. Control. Release* **70**: 1–20

Subramanian, A., Hommerding, J. (2005) The use of confocal laser scanning microscopy to study the transport of biomacromolecules in a macroporous support. *J. Chromatogr. B* **818**: 89–97

Tuma, R. (2005) Raman spectroscopy of proteins: from peptides to large assemblies. *J. Raman Spectrosc.* **36**: 307–319

Ulbrandt, N. D., Cassatt, D. R., Patel, N. K., Roberts, W. C., Bachy, C. M., Fazenbaker, C. A., Hanson, M. S. (2001) Conformational nature of the *Borrelia burgdorferi* decorin binding protein A epitopes that elicit protective antibodies. *Infect. Immun.* **69**: 4799–4807

Vangala, A., Bramwell, V. W., McNeil, S., Christensen, D., Agger, E. M., Perrie, Y. (2007) Comparison of vesicle based antigen delivery systems for delivery of hepatitis B surface antigen. *J. Control. Release* **119**: 102–110

Vila, A., Sanchez, A., Janes, K., Behrens, I., Kissel, T., Jato, J. L. V., Alonso, M. J. (2004) Low molecular weight chitosan nanoparticles as new carriers for nasal vaccine delivery in mice. *Eur. J. Pharm. Biopharm.* **57**: 123–131

Wang, W. (1999) Instability, stabilization, and formulation of liquid protein pharmaceuticals. *Int. J. Pharm.* **185**: 129–188

White, K., Rades, T., Kearns, P., Toth, I., Hook, S. (2006) Immunogenicity of liposomes containing lipid core peptides and the adjuvant Quil A. *Pharm. Res.* **23**: 1473–1481

Yamasaki, M., Takahashi, N., Hirose, M. (2003) Crystal structure of S-ovalbumin as a non-loop-inserted thermostabilized serpin form. *J. Biol. Chem.* **278**: 35524–35530

Zaharoff, D. A., Rogers, C. J., Hance, K. W., Schlom, J., Greiner, J. W. (2007) Chitosan solution enhances both humoral and cell-mediated immune responses to subcutaneous vaccination. *Vaccine* **25**: 2085–2094

Zhao, Z., Leong, K. W. (1996) Controlled delivery of antigens and adjuvants in vaccine development. *J. Pharm. Sci.* **85**: 1261–1270

Zinkernagel, R. M., Ehl, S., Aichele, P., Oehen, S., Kündig, T., Hengartner, H. (1997) Antigen localisation regulates immune responses in a dose- and time-dependent fashion: a geographical view of immune reactivity. *Immunol. Rev.* **156**: 199–209